Cosmic Ray Muon Detection using NaI Detectors and Plastic Scintillators

Chung Yau Elton Ho

Abstract

We measured the zenith angle θ distribution of cosmic ray muons at ground level using NaI detectors and plastic scintillators, and our data is consistent with the $\cos^2\theta$ distribution obtained from theory and other experiments. We also discussed the pros and cons of using NaI detectors and plastic scintillators.

Contents

1 Introduction

At sea-level the incident angle of cosmic ray muons typically follow a $\cos^2\theta$-distribution, where θ is the zenith angle. In our experiment we utilized two different types of detectors, NaI detectors and plastic scintillators, to measure this distribution.

2 Theory

2.1 Cosmic Ray Muons

Cosmic rays are often defined as charged particles that reach the Earth from interstellar space. As particles arrive at Earth's atmosphere, they interact with the atoms and molecules present, producing secondary particles that continue to propagate towards the Earth surface. These interactions can occur multiple times before a particle reaches sea level, while some particles can be stopped during its path through the atmosphere. This collective flux of primary, secondary, tertiary, etc. particles are typically referred to as air showers or cosmic ray showers. For the sake of consistency, we shall refer to this flux of particles as cosmic rays throughout this article.

The abundance of each species of particles in atmospheric cosmic rays is energy dependent. On the average the relative abundances are as follows: protons $\sim$ 89 %, helium $\sim$ 9 %, electrons $\sim$ 1 %, heavy nuclei $\sim$ 1 % and some minor presence of other particles [5]. However, at sea level muons are one of the most abundant energetic particles. In the atmosphere high-energy primary nuclei interacts with atmospheric ones, which produces pions and kaons. These particles decay into muons through the following mechanisms:

$$\pi^- \to \mu^- + \bar{\nu}_\mu \tag{1}$$

$$K^- \to \mu^- + \bar{\nu}_\mu \tag{2}$$

The muon is a second-generation elementary particle in the lepton sector. It carries a negative charge with half spin, and has a mass of approximately 105.658 MeV, which is over 200 times heavier than the electron. The muon is unstable, and has a life-time of 2.2 μs [2]. The most common decay mode of a muon is through the following:

$$\mu^- \to e^- + \bar{\nu}_e + \nu_\mu \tag{3}$$

Despite being unstable, due to its heavy mass, muons have high penetrating power. Although muons have a short life-time, ones that are produced at the top of the atmosphere can travel through the atmosphere and reach sea level due to that they travel at relativistic speeds with high energy.

During its time of flight, muons can lose energy through Coulomb scattering, ionization loss, Compton scattering and Bremsstrahlung. Since muons are massive, they mostly only lose energy through ionization. On the average cosmic ray muons lose 2 GeV throughout their course towards sea level to ionization [1]. Upon reaching ground, the energy spectrum of muons are analytically derived as Eq. (4) and experimentally shown in Fig. 1.

$$\frac{dN_\mu}{dE_\mu d\Omega} \approx 0.14E_\mu^{-2.7}[\text{cm}^2\text{ s sr GeV}]^{-1} \times \left[\frac{1}{1+\frac{1.1E_\mu\cos\theta}{115\text{GeV}}} + \frac{0.054}{1+\frac{1.1E_\mu\cos\theta}{850\text{GeV}}}\right] \tag{4}$$

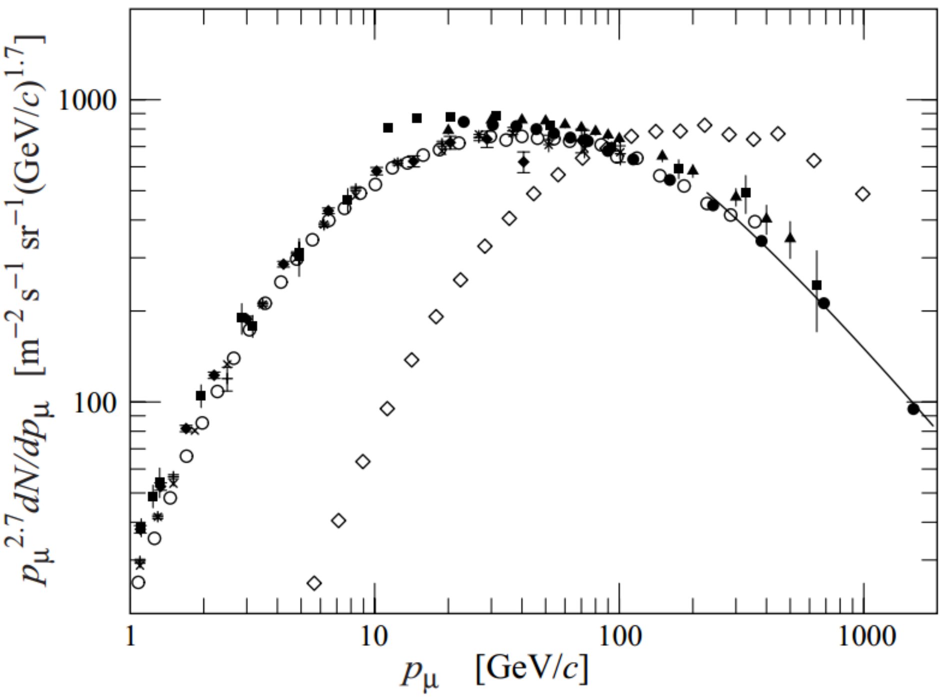

Figure 1: Spectrum of muons at $\theta = 0°$ with the exception that hollow diamond markers represent data at $\theta = 75°$. Different markers represent data obtained from different experiments. The solid line plots Eq. (4). This graph is obtained from the particle data group [1].

The flux of cosmic ray muons depends on the incident zenith angle. In particular, the relation is

$$I(\theta, h, E) = I(0°) \cos^{n(E,h)}(\theta) \tag{5}$$

where θ is the zenith angle, h is the vertical distance traveled by the muon, E is the energy of the muon, and $n(E, h)$ is an empirically determined constant. At sea level experiments showed that $n \approx 2$. In our experiments we are going to show that indeed the cosmic ray muon flux has a $\cos^2 \theta$ distribution.

2.2 Muon Interaction with Matter

In order to understand the working principle of scintillation detectors, we need to discuss the processes that occur when muons pass through and interact with matter.

When a charged particle passes through matter, it can lose energy and be deflected from its incident direction. For charged heavy particles, such as muons, these effects are primarily due to inelastic collisions with atomic electrons of the material. The amount of energy transferred during every collision is small, but in dense media the interaction cross section can be large and many collisions can occur per path length, so the cumulative effect can lead to substantial energy loss.

A quantum-mechanical description of how this energy loss relates to its relevant quantities is shown mathematically by the Bethe-Bloch formula that describes the stopping power of a material for different incident particles. For experimental purposes this formula was slightly altered to include realistic experimental effects. The following is the formula:

$$-\frac{dE}{dx} = 2\pi N_a r_e^2 m_e c^2 \rho \frac{Z}{A}\frac{z^2}{\beta^2}\left[\ln\left(\frac{2m_e\gamma^2 v^2 W_{max}}{I^2}\right) - 2\beta^2 - \delta - 2\frac{C}{Z}\right] \tag{6}$$

with

$$2\pi N_a r_e^2 m_e c^2 = 0.1535 \text{ MeV cm }^2/\text{g} \tag{7}$$

r_e: classical e^- radius $= 2.817 \times 10^{-13}$ cm
m_e: electron mass 0.511 MeV/c^2
N_a Avogadro's number $= 6.022 \times 10^{23}$
I: mean excitation potential
Z: atomic number of absorbing material
A: atomic weight of absorbing material
W_{max}: maximum energy transfer in a single collision
ρ: density of absorbing material
z: charge of incident particle in units of e
β: v/c of the incident particle
γ: $1/\sqrt{1-\beta^2}$
δ: density correction
C: shell correction

The maximum energy transfer is produced by a knock-on collision[1]. For an incident particle of mass M,

$$W_{max} = \frac{2m_e c^2 \eta^2}{1 + 2s\sqrt{1+\eta^2} + s^2} \tag{8}$$

where $s = m_e/M$, M is the mass of an incident particle, and $\eta = \beta\gamma$. For the case of muons, since the mass of a muon $M = m_\mu$ is much greater than the mass of an electron m_e, we have

$$W_{max} \approx 2m_e c^2 \eta^2 \tag{9}$$

The mean excitation potential I is theoretically a logarithmic average of electron bound state frequencies weighted by the oscillator strengths of the atomic levels. However, this quantity is very hard to calculate in reality. Its value is usually determined empirically.

The electric field of the incident particles tends to polarize atoms in the material, leading to a density correction term δ. The polarization of atoms near the path of the traveling particle shields off electrons far away from the full electric field intensity. Collisions with the outer lying electrons will contribute less to the total energy loss. This effect increases with increasing incident particle energies and material density.

The shell correction C accounts for effects which arise when the velocity of the incident particle is comparable or smaller than the orbital velocity. The electrons in the material can no longer be treated as stationary in this energy regime.

The Bethe-Bloch formula is plotted in Fig. 2 as a function of momenta of incident particles. The curve is decreasing at lower energies until a certain point where the curve becomes relatively constant. Particles at these momenta where the value of dE/dx is minimal are call minimum ionizing particles. Their energy deposition per unit distance traveled over a piece of material is relatively constant. Cosmic ray muons travel at relativistic speeds at ground level, and are typically minimum ionizing particles. A commonly used approximation for dE/dx is 2 MeV/(g/cm^2).

[1] Knock-on or hard collisions are those in which energy transfer from the incident particle is sufficient to cause ionization of the atoms in the target material.

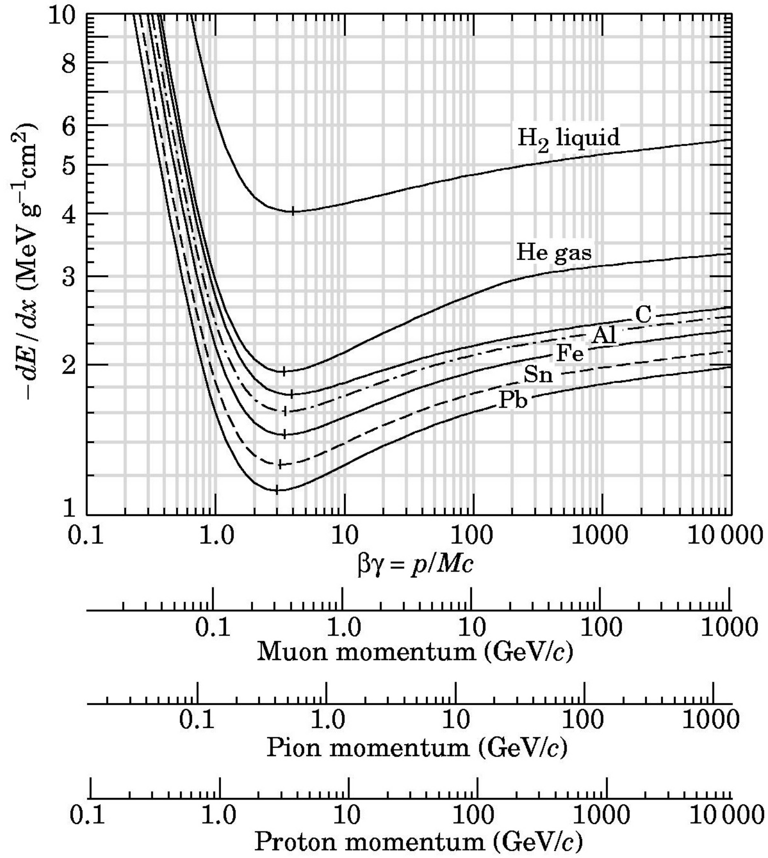

Figure 2: Energy dependence of the energy deposition per distance traveled of different charged particles in different media.

3 Apparatus

3.1 Scintillation Detectors: NaI crystals and polystyrene

When certain particles or radiation pass through matter, they excite the atoms and molecules in the target material which causes light emission, or, in other words, scintillation. Through collecting and analyzing the light produced, we can extrapolate the species of particles that caused the emission.

The use of scintillation detectors for our purposes mainly has two advantages.

First, it is sensitive to energy. In cosmic ray showers there are particles that come in different energy ranges. Muons, with their characteristically high energies at ground level, can be easily distinguished from other particles by most energy-sensitive detectors.

Moreover, it provides fast response. This gives a better resolution to particles incident on the material since the overlapping time between light produced by different particles is minimized. More particles can then be differentiated, which leads to a higher probability in obtaining a pure signal produced solely by muons.

Both NaI and polystyrene are luminescent materials. When being exposed to certain energies sources, they absorb the energy and re-emit in the form of light. To first order the rate of re-emission is directly proportional to the number of excited atoms and molecules. Therefore such emission follows a simple exponential decay. For higher accuracy we can further approximate the emission as a superposition of different decay modes with distinct decay life-time. Due to exponential decay during emission, the output signal from a scintillator resembles such shape, and can be observed through direct measurement.

We now compare the pros and cons of using NaI crystals and plastic.

NaI is one of the most widely used inorganic crystals for scintillation purposes. Inorganic crystals usually have greater stopping power due to their high density and atomic number. This translates into higher light output for the same volume of materials used, resulting in better energy resolution. Typically the response of NaI is on the order of 10 μs, and is slower than that of organic scintillators, such as plastic, by 2-3 orders of magnitude due to phosphorescence[2]. The scintillation mechanism is mainly due to electronic band structure effect. During excitation, an electron can be excited from a non-conducting band to a conducting band or another non-conducting band that is close to a conducting band. The latter is called an exciton. When an electron is excited into the conducting band as a free electron, a free hole is created in the crystal. In the exciton an electron binds with a hole to form a freely moving pair. For either case of the free hole and exciton, when it encounters an impurity center in an impurity atom, the atom ionizes. When another electron passes through the ionized atom, the electron de-excites and drops into the hole of the ionized atom. This de-excitation causes the scintillation in NaI crystals. The amount of light produced follows an exponential decay since the rate of de-excitation is proportional to the number of excited states.

Plastic scintillators are probably the most widely used organic detectors, and polystyrene is one of the most widely used materials in the making of plastic detectors. In contrary to inorganic scintillators, plastic scintillators provide extremely fast response but less efficiency. Common response times range from a couple to tens ns. Only fluorescent light is produced during excitation of molecules, and phosphorescence does not occur, which leads to such fast response. The light produced is mainly from transitions made by free valence electrons of the plastic molecules. These electrons are excited in the π-moelcular orbitals. For each electron level there exists a fine structure which corresponds to excited vibrational levels. Both of these excited levels can de-excited and emitted light. Since the rise and decay time for scintillation in these scintillators are very fast, the intensity of light produced does not follow a simple exponential decay. Instead it takes the form of an exponential decay convoluted by a Gaussian curve.

3.2 Nuclear Instrument Module (NIM) Electronics

The Nuclear Instrument Module (NIM) standard is adopted worldwide by laboratories and commercial enterprises as a standard for electronics. A typical NIM system set-up consists of a series of NIM modules, which can perform a variety of functions, and a NIM bin, which provides power supply to the modules.

Most power bins provide voltages of ± 24 V and ± 12 V, while some also provide additional ± 6 V pin-outs. Most modules require a specific configuration of voltage supplies. For example, some discriminators require a ± 6 V pin-out from the power bin, which means that not all bins would be able to power the chosen discriminator.

The NIM modules that we used during our experiments are Canberra amplifier model 2022, single channel analyzer model 2037A, coincidence unit 2040, counter timer 2071A, a Philips Scientific discriminator 730, and a LeCroy 4-fold logic unit. These electronics are shown in Fig. 3, 4 5, and 16. In the following we will discuss the usage of such modules specifically for our experimental set-up.

[2] If an excited atom or molecule is metastable, it takes more time for light to be emitted. This is referred to as phosphorescence.

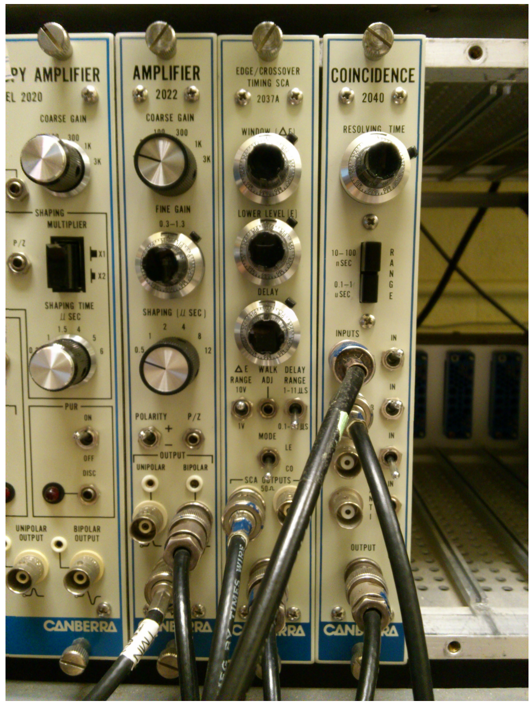

Figure 3: A Canberra amplifier model 2022, single channel analyzer (SCA) model 2037A, and coincidence module model 2040.

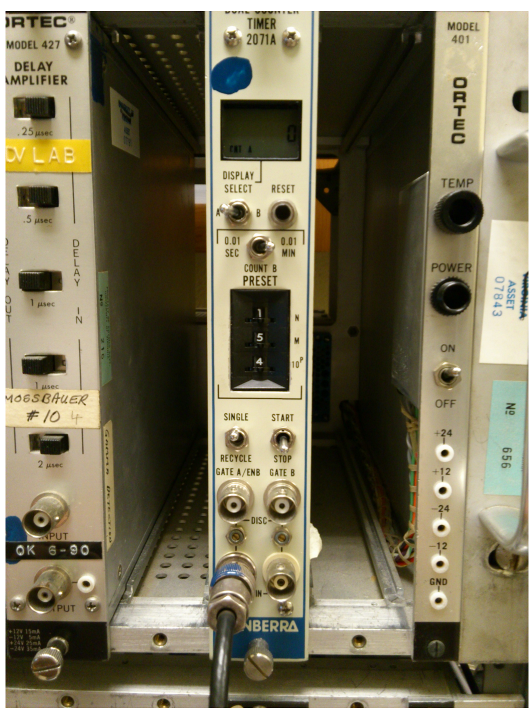

Figure 4: A Canberra counter timer 2071A.

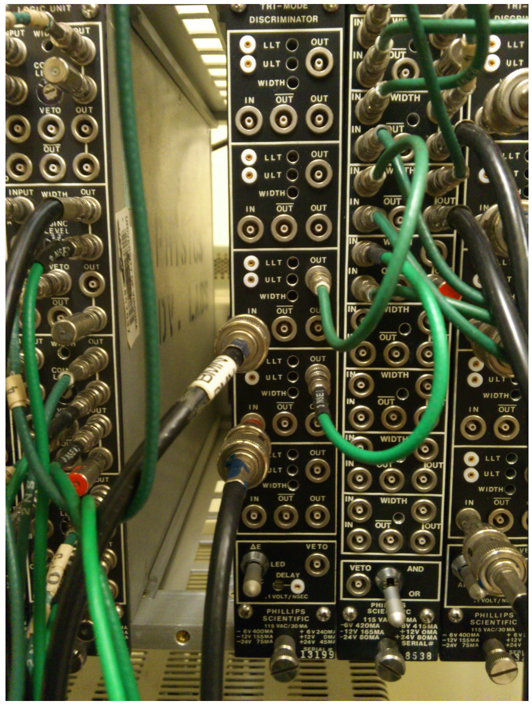

Figure 5: A PS discriminator 730.

Amplifier. When an amplifier takes in a signal pulse, it amplifies and reshapes the pulse. The amplification can range from three to a couple thousand, and the pulse width can be changed within the μs range to suppress electronic noise. There are two output choices: unipolar and bipolar. We chose bipolar for our experiments. This setting gives us an output pulse that has both a positive and negative component to it. This type of pulse works for some electronics that only take in a particular polarity on top of regular modules.

Single channel analyzer and discriminator. Single channel analyzers (SCA) and discriminators are used to select signals with desired voltages and delaying signal outputs. A lower energy threshold (E) is set so that all pulses with voltage less than E will be ignored. An energy window (ΔE) can also be set so that a voltage upper limit at $E + \Delta E$ prevents signals with higher voltage from passing. When multiple channels are used to find signal coincidences in a coincidence unit, a delay is usually applied to line up different signal pulses in the single channel analyzer or discriminator. Single channel analyzers can only take in one input, while discriminators can usually filter multiple inputs at the same time.

Coincidence and logic unit. A coincidence, or logic, unit takes in multiple inputs. Whenever pulses from these inputs arrive at the unit within a pre-decided time window, the unit produces a logic pulse at its output. For a more accurate measurement of coincidences, the time window is usually chosen to be minimal with input pulses being pre-aligned before channeling into the unit.

Counter. A counter timer counts the number of positive logic pulses that are input. Two modes can be chosen: fixed time and fixed count. For our experiment the better choice was to set a very long fixed time, and when we need to terminate data acquisition, we can manually stop the counter. This can provide more statistics to out results.

3.3 Photomultiplier Tubes

Photomultiplier tubes (PMT) bridge the production of light by scintillators and the analysis by NIM modules through converting light into measurable electron current.

The schematic of a PMT is shown in Fig. 6. Its major internal components include a photocathode, focusing electrodes, an electron multiplier (dynodes) and an anode. The outer case is usually an evacuated glass tube.

When light passes through the faceplate and hits on the photocathode, the electrons in the photocathode are excited so that photoelectrons are emitted. This process is called external photoelectric effect. The kinetic energy of photoelectrons escaping is described by Einstein's Nobel-Prize-winning yet simple formula:

$$E = h\nu - \phi \tag{10}$$

where h is Planck's constant, ν is the frequency of the incident light, and ϕ is the work function specific to the material making up the photocathode. Most photocathodes are made of semiconductors, which are efficient in carrying out photoelectric effect. The ratio of output electrons to incident photons is called the quantum efficiency, and is given by

$$\eta(\nu) = (1 - R)\frac{P_\nu}{k}\left(\frac{1}{1 + 1/kL}\right)P_s \tag{11}$$

R: Reflection coefficient
k: Full absorption coefficient of photons
P_ν: Probability that light absorption may excite electrons
L: Mean escape length of the excited electrons
P_s: Probability that electrons reaching the photocathode surface is released
ν: frequency of light

After photoelectrons are produced at the photocathode, an electron-optical input system is used to generate a magnetic field that focuses the photoelectrons onto a single dynode. Good systems tend to be efficient in photoelectron collection and has a well-defined time-of-flight for photoelectrons to reach the dynode regardless of the point of generation.

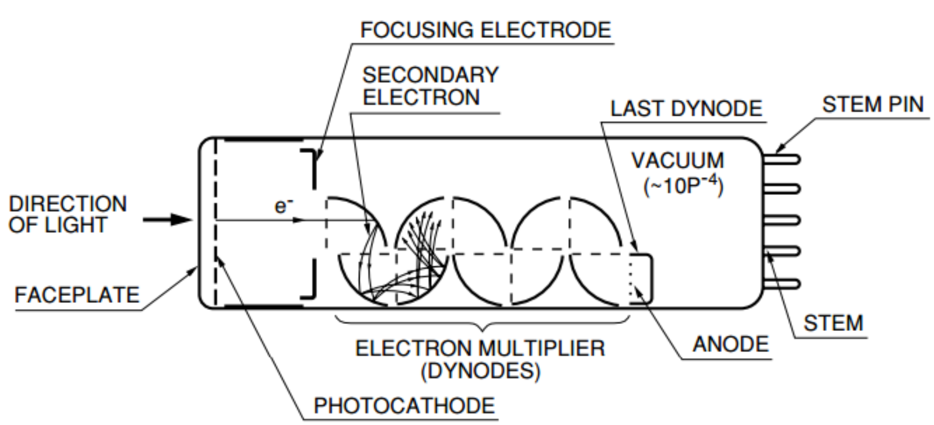

Figure 6: Construction of a photomultiplier tube (PMT).

As photoelectrons strike a dynode, which are also called secondary emission electrodes, secondary emission of multiple electrons is induced. The gain in the number of electrons at each electrode is called the secondary emission ratio/factor. In a typical PMT there are can be 10 to 108 dynodes. The process of secondary emission is similar to that of the photoelectric effect but with photons replaced by electrons. In order to guide the electrons towards the anode, voltage is supplied to each dynode through a voltage divider. Usually a high negative voltage at around 1500 kV to 2000 kV is applied at the first dynode, and the voltage of the last dynode is set to nearly zero.

After the last dynode, electrons are ejected at the anode. To read out the signal of the PMT, the anode can be connected to any other desired devices such as an oscilloscope or an analyzer.

4 Detection using NaI Detectors

4.1 Set-up

The set-up for the experiment is shown in Fig. 7 and 8.

NaI crystal detectors are attached to a photomultiplier tube (PMT) with an attached pre-amplifier base. Two sets of detectors are aligned as shown in Fig. 9. The separation between detectors are maintained at $D = 5$cm, while the zenith angle θ is varied to measure the angular distribution of cosmic ray muons.

A voltage of ~ 2000 V is applied to each of the PMT's. The signal produced at the PMT's is channelled to an amplifier, and is re-shaped as a bipolar pulse. Practically only muons can both produce high energy pulses and a coincidence at the same time[3], and therefore the lower energy edge and the ΔE window of the single channel analyzer (SCA) are set to their maximum values to sample high energies. The bipolar pulse is analyzed by the SCA, and only high energy signals are passed to the coincidence unit. The coincidence time window is set to 100 ns, which is the lower limit. The signal channelled out from the coincidence unit is counted by a counter, and the number of counts are recognized as the number of cosmic ray muons passing through both of the detectors.

4.2 Signal Output

Figure 10 shows a raw signal output at the anode of one PMT caused by a cosmic ray muon being detected by a NaI detector. The pulse has a negative amplitude because electrons are expelled from the anode of the PMT and reaches the oscilloscope as a negative current. Notice that the time scale on the oscilloscope is set to 40 μs, which indicates a long de-excitation time needed for NaI to resolve a detection of a cosmic ray muon.

We now use both NaI detectors. After we attached a pre-amplifier to each of the PMT's, the polarity of the signal pulse is flipped, as shown in Fig. 11. The figure shows the pulse shape of a muon event. Both detectors observed a strong pulse within a very short time window. This suggests a high probability that some energetic particle passed through and deposited energy in both detectors. Since muons are almost the only cosmic ray particle that can cause such response to these detectors at ground level, we register this event as being caused by a cosmic ray muon.

[3] An air shower can produce a large number of particles that reach both of out detectors at nearly the same time. The signal generated can look like coincidence events, but are caused by the detection of two different particles. These events have low energies compared to muon events, and therefore a lower threshold can be introduced to filter out low-energy pulses.

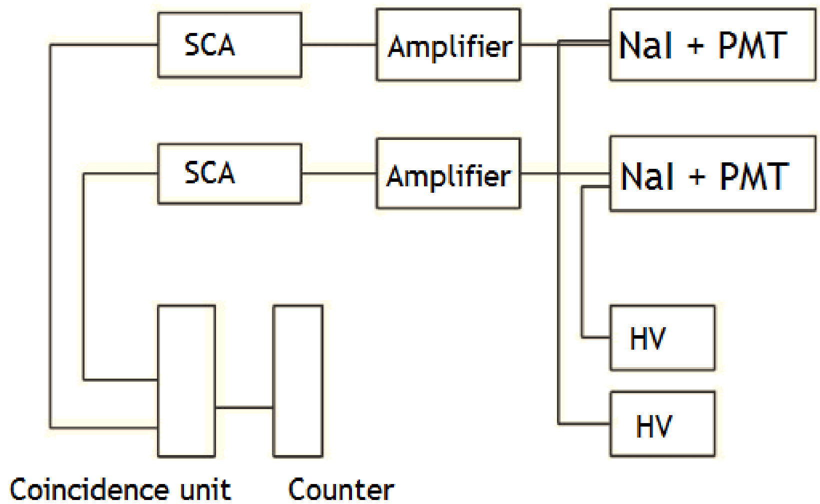

Figure 7: A schematic outline of the set-up. SCA refers to a single channel analyzer; HV refers to a high voltage supply; PMT refers to a photomultiplier tube together with a NaI crystal detector and a pre-amplifier base.

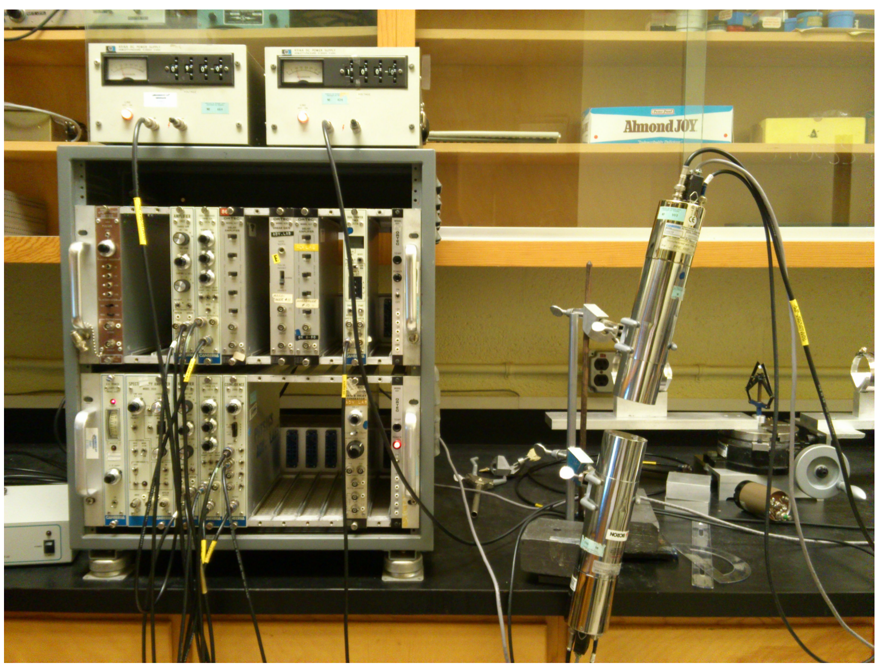

Figure 8: Set-up of the experiment.

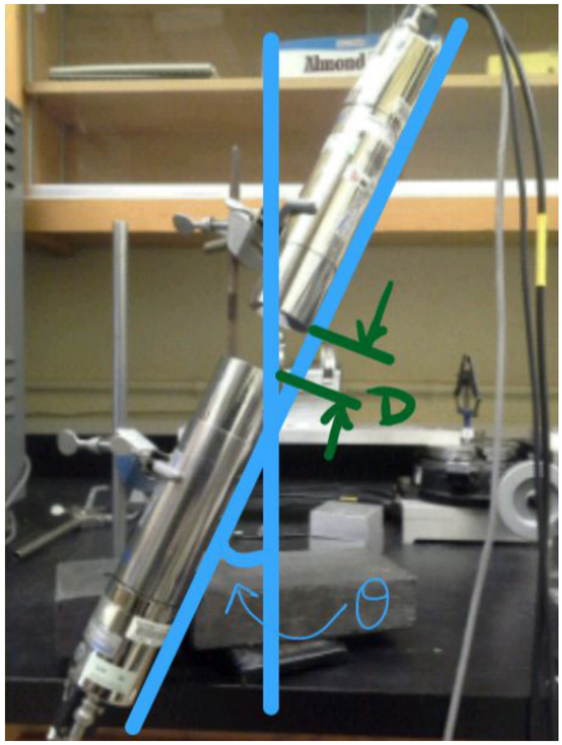

Figure 9: Separation D between detectors and the alignment of detectors with the zenith angle *theta*.

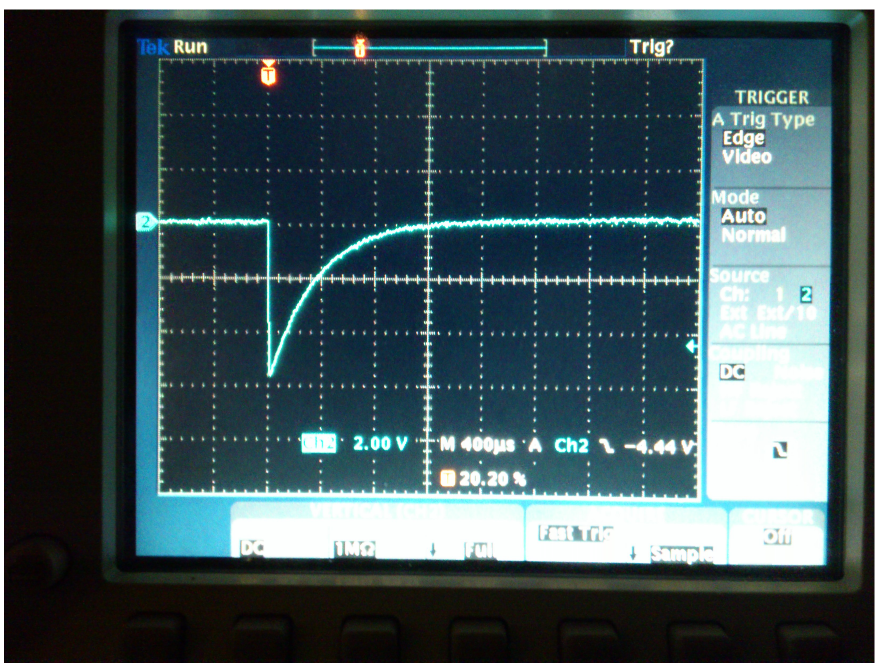

Figure 10: Signal output due to the detection of a cosmic ray muon from the anode of a PMT.

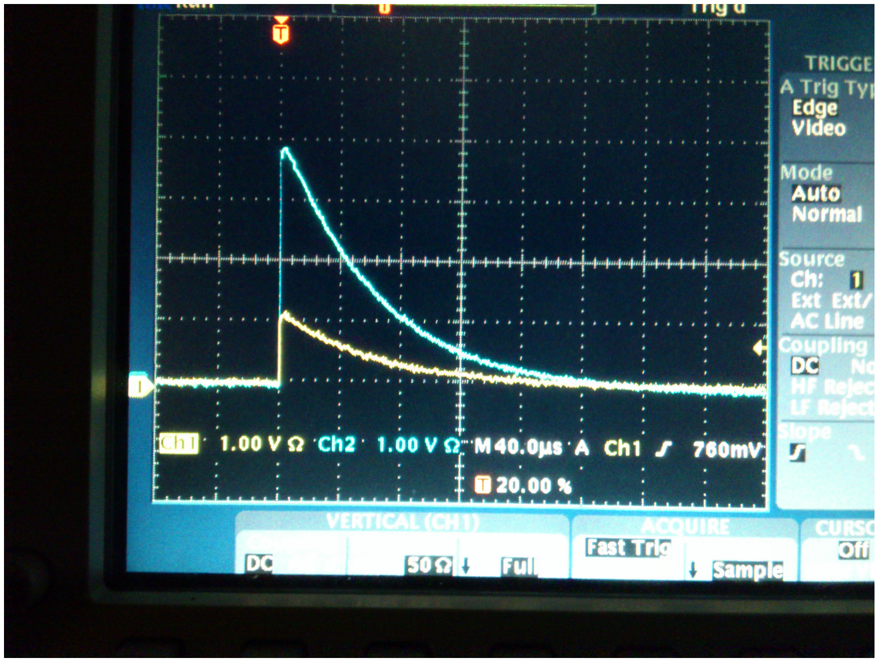

Figure 11: Signal output due to the detection of a cosmic ray muon from two PMT's each attached with a pre-amplifier .

4.3 Results

After taking measurements at nine different zenith angles θ, we obtained the data shown in Fig. 12. The data is fitted with a function of the form $A\cos^2(2\pi\theta/360°) + B$, where A and B are fitting parameters, and θ is measured in units of degrees. Due to the set-up of the detectors, we should not expect a bias in the measurement of the zenith angle towards a more positive or negative angle, and therefore no fitting parameter is involved within the argument of the cos term, i.e. no phase shift parameter is introduced. Vertical errors bars indicate statistical errors due to statistical fluctuations, while horizontal error bars show the measurement errors in the zenith angle. Other experimental errors are not shown in the error bars. The $\pm\sigma$ fit lines are constructed by varying both of the fit parameters to one standard deviation away from the fitted value and replacing A and B in the fit function with the altered value.

Our measured data are mostly within one statistical standard deviation from the best fit curve, indicating good consistency with theory and experiment results produced in other studies. The best fit parameters are obtained as $A = (290.8 \pm 5.0) \times 10^{-4}$ and $B = (39.4 \pm 2.7) \times 10^{-4}$. A is used to account for normalization; B is included to adjust for constant background and systematic errors. The residual after fitting is shown in Fig. 13. All data lie within one statistical standard deviation from the fit function, while all error bars also lie within one parameter standard deviations. The χ^2 and reduced χ^2 are calculated to be 1.7821 and 0.25459 respectively. A reduced χ^2 less than one suggests that the fit is reliable and the errors we considered are the dominating uncertainties.

Experimental errors mainly arise from aligning the detectors and measuring the exact zenith angle. A rough estimation to the these errors are $\theta \pm 1°$ and $D \pm 0.2$cm.

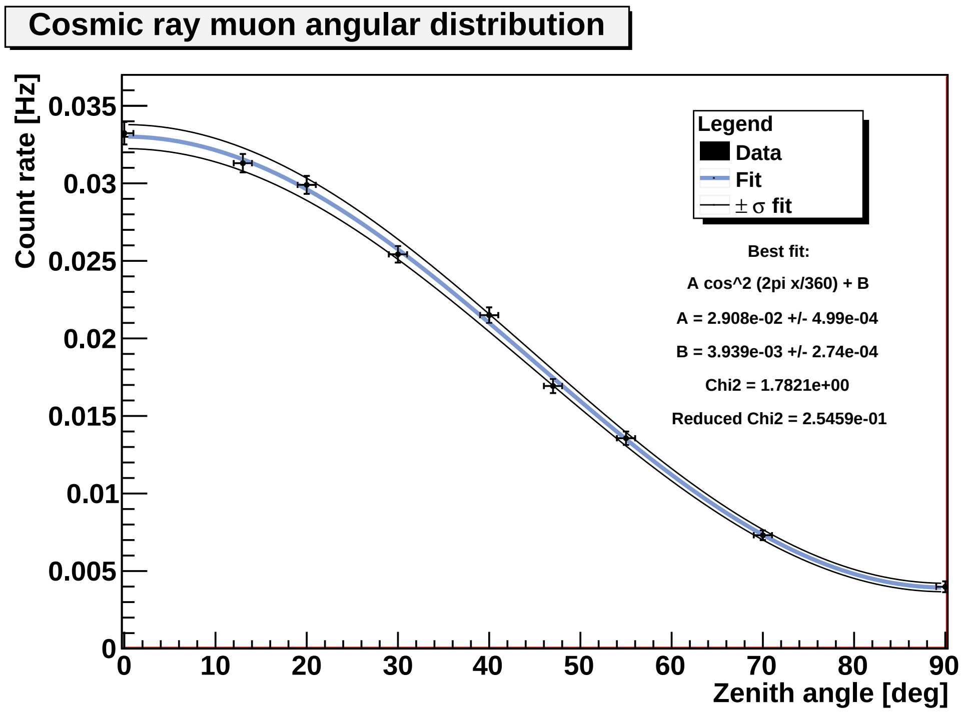

Figure 12: Angular distribution of cosmic ray muons as measured using coincident method.

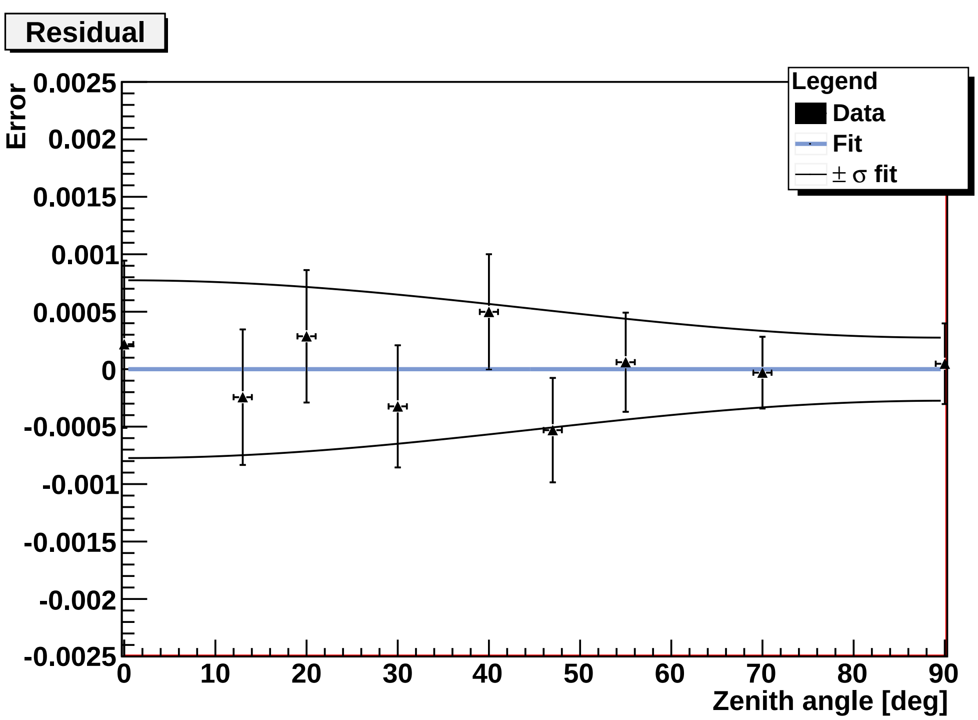

Figure 13: Residual after fitting.

5 Detection using Plastic Scintillators

5.1 Set-up

The set-up for the experiment is shown in Fig. 14, 15 and 16.

Plastic scintillators with attached PMT's are aligned so that they are separated by approximately $D = 23$ cm. The zenith angle θ is measured in the same way as in the previous experiment. Here this angle is that between the normal to the scintillator paddles and the vertical.

Signal is extracted out from the anode of the PMT, and relayed to a discriminator. The lower energy edge E of the discriminator is set to its maximum value, and the ΔE window is disabled, so that all pulses with energy greater than E is accepted. We have pulse width of the output signal to $\sim$ 40 ns. The signals from the discriminator are passed to the logic unit. The coincidence unit, instead of using a coincidence window, determines if two pulses overlap and produces a logic signal for every overlapping pulse event. Here since the input pulse width is 40 ns, it is equivalent to having a 80 ns coincidence time window. The signal channelled out from the coincidence unit is passed through an amplifier. An amplifier is needed here to convert the signals into bipolar pulses, which can be counted by a counter, and the number of counts are registered as the number of cosmic ray muons passing through both of the detectors.

5.2 Signal Output

Figure 17 shows the signal output of a coincidence event at the anode of both PMT caused by a cosmic ray muon passing through both scintillators. The operational principle of plastic scintillators is essentially the same as the NaI detectors we used previously. Therefore, we have electrons ejected from the anode, causing the negative pulse, and have a high confidence in identifying this signal as a muon event. Notice that the time scale on the oscilloscope is now set to 10 ns, which indicates a very short de-excitation time needed for plastic scintillators to resolve a detection of a cosmic ray muon, relative to that of NaI detectors ($\sim 40\mu$s).

5.3 Results

Ten data points were measured at ten different zenith angles θ, and the plot as shown in Fig. 18 is produced. Same as the NaI detectors, we fitted the data with a function of the form $A\cos^2(2\pi\theta/360°)+B$, where A and B are fitting parameters, and θ is measured in units of degrees. No phase shift parameter is included in the argument of the cos term. The vertical and horizontal error bars indicate statistical errors in the count rate and measurement errors in the zenith angle respectively. We produced the $\pm\sigma$ lines by increasing/decreasing both of the fit parameters at the same time to one standard deviations away from the fitted value.

Our data shows some consistency with theory and experiment results produced in other studies. In particular we can observe a $\cos^2\theta$ zenith angular distribution. The best fit parameters are obtained as $A = (438.0 \pm 7.0) \times 10^{-3}$ and $B = (179.9 \pm 2.1) \times 10^{-3}$. The residual after fitting is shown in Fig. 19. Some data points lie more than three statistical standard errors in the vertical, but all data lie with three standard errors when horizontal errors are considered. The χ^2 and reduced χ^2 are calculated to be 21.652 and 2.7065 respectively. A reduced $\chi^2 > 2$ suggests that there are some errors that we have not included in our data.

Apart from errors in aligning the detectors ($\pm$ 0.5 cm)and measuring the exact zenith angle ($\pm$ 2°), a major error is the geometric effect caused by the comparable length scales between the separation between scintillators ($\sim$ 23 cm) and the width of scintillators ($\sim$ 18 cm). With this geometry the experiment surveys

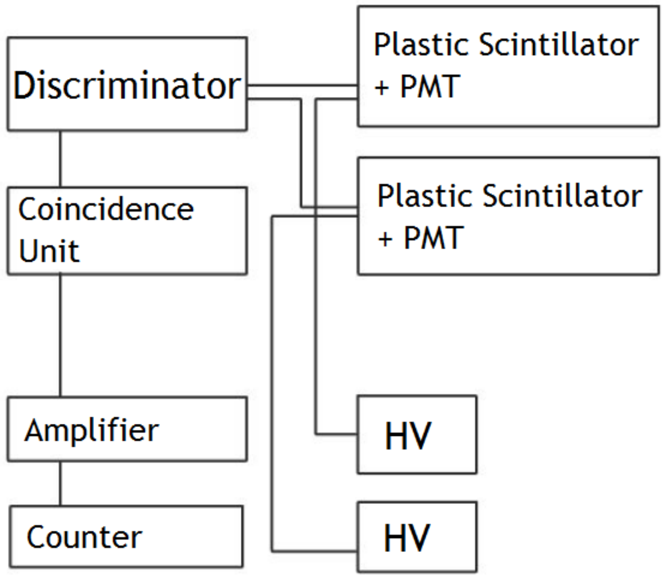

Figure 14: A schematic outline of the set-up. HV refers to a high voltage supply.

Figure 15: Plastic scintillator paddles used.

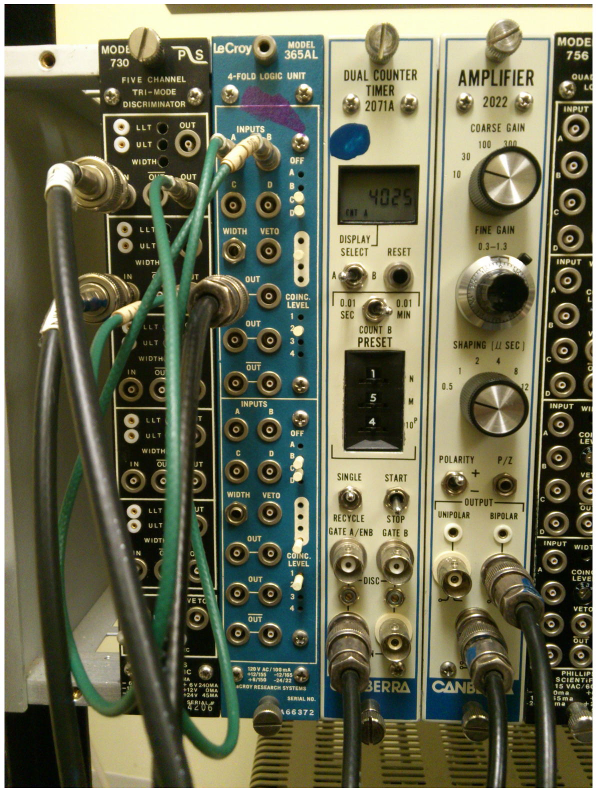

Figure 16: NIM modules used for this experiment.

Figure 17: Signal output due to the detection of a cosmic ray muon.

a range of zenith angles, instead a well-defined one. This effect can be further investigated to improve the experiment.

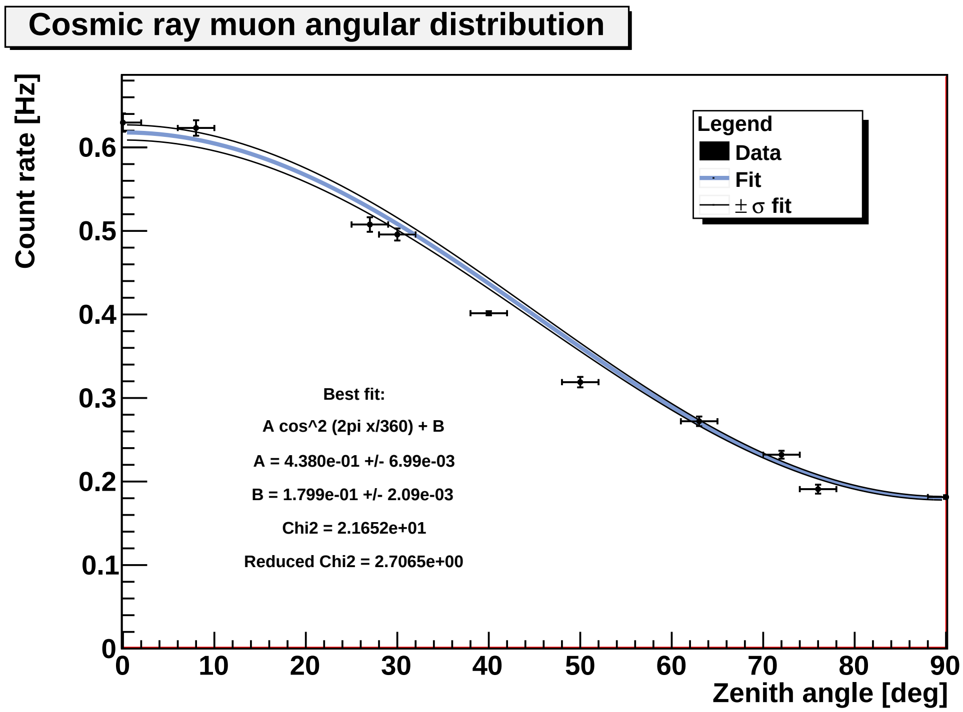

Figure 18: Angular distribution of cosmic ray muons as measured using coincident method.

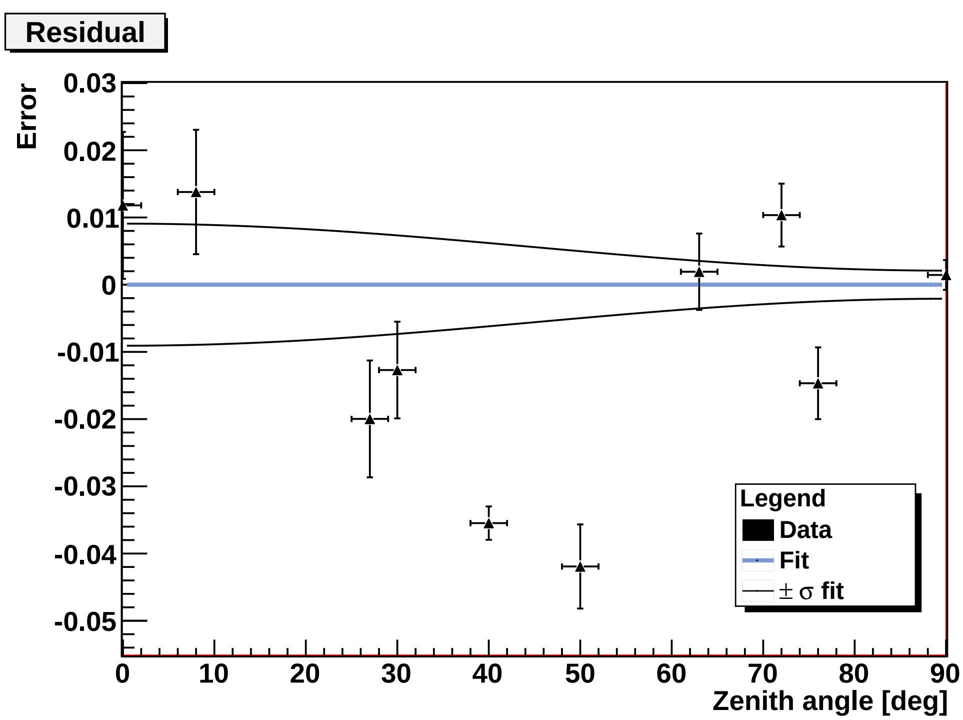

Figure 19: Residual after fitting.

6 A Short Comparison between NaI Detectors and Plastic Scintillators

This section focuses on the experimental difficulties and merits that I encountered during the use of NaI detectors and plastic scintillators.

NaI detectors have, in general, better structural integrity over plastic scintillators. NaI detectors are usually housed in a metal case when they are produced which give them a very rigid shape. Plastic scintillators, on the other hand, are more flexible, and can bend significantly under gravity. This makes aligning NaI detectors easier than plastic scintillators.

NaI detectors are usually light-tight as they are manufactured with the metal case being the light shield. Plastic scintillators are typically wrapped in layers of aluminum foils with an outer layer of tape to shield off ambient light. Aluminum foil can be damaged under the tape, while leaving no evidence of damage on the outer surface of the scintillator. Searching for potential light leaks is a difficult task, and it might be easier to simply wrap another layer of light-isolation material on top to reduce light leaks. This makes NaI detectors more reliable in detecting muons. However, it is difficult to fix a NaI detector when light leak occurs.

The data collection rate of plastic scintillators is much higher than that of NaI detectors. Inorganic crystals are in general very difficult to grow more than a couple centimeters, while plastic scintillators can be made, in principle, up to some meters. In our experiments, in order to obtain the same number of muon counts, NaI detectors require around 13 to 15 times the time needed for plastic scintillators.

7 Conclusion

We have demonstrated that cosmic ray muons at ground level have a $\cos^2\theta$ zenith angle distribution, using NaI detectors and plastic scintillators. Both types of detectors showed consistent results. We further discussed the merits of using each of the detectors.

For future improvements, we can investigate how geometric effects can affect detector performances and count rates.

A Program used for Fitting Data

ROOT was used to fit the data. The ROOT library, a C/C++ library developed by CERN, is a powerful data analysis tool designed to manipulate large amounts of data. It provides routines in performing complicated math operations, information handling, data fitting, etc.

In my program I mainly used the TGraphErrors class to store my experimental data and the TF1 class to input my function for fitting. The essential lines of code are presented below. Note that this code is used for fitting the data collected by plastic scintillators. The code used for the NaI detector data is very similar with minor changes that do not affect our discussion here.

```
#include "TF1.h"
#include "TGraphErrors.h"
...
const Int_t size = 10;
```

```
const char* inputName = "inputP.dat";
...
void plasticData(){

  //Read in data from external file ‘‘inputP.dat’’
  //The number of lines read in is limited by ‘‘size’’
  //  x[],y[] -> Data: angle and count rate
  //  xerr[], yerr[] -> Errors in data

  FILE *inFile = fopen(inputName,"r");
  Double_t x[size],y[size],xerr[size],yerr[size];
  for(Int_t i=0; i<size; i++){
    xerr[i]=2;
    fscanf(inFile,"%lf %lf %lf",&x[i],&y[i],&yerr[i]);
    printf("%e %e %e\n",x[i],y[i],yerr[i]);
  }

  //Set up TGraphErrors object ‘‘graph’’ to hold data and
  //TF1 object ‘‘fitFunc’’ to carry the fit function.

  TGraphErrors *graph = new TGraphErrors(size,x,y,xerr,yerr);
  TF1 *fitFunc = new TF1("fitFunc","[0]*cos(pi*x/180)*cos(pi*x/180)+[1]",0,90);

  //Fitting and extracting chi2 and reduced chi2

  graph->Fit(fitFunc,"R0FMV");
  printf("Chi2 = %e\n",fitFunc->GetChisquare());
  printf("Reduced Chi2 = %e\n",fitFunc->GetChisquare()/fitFunc->GetNDF());
...
}
```

References

[1] J. Beringer et al. (Particle Data Group) PR D86, 010001. (2012)

[2] D. Denisov *Detection of Muons.* Academic Lecture. April, 2000.

[3] J. Kempa and I. M. Brancus. Nuclear Physics B (Proc. Suppl.) 122 (2003) 279-281

[4] W. R. Leo *Techniques for Nuclear and Particle Physics Experiments.* Springer, 1994.

[5] G. Micheva *Cosmic Ray Composition.* Lecture notes. September, 2007.

[6] T. Stanev *High Energy Cosmic Rays.* Springer & Praxis, 2010.

[7] *Experiments in Nuclear Science.* ORTEC, July, 1976.

[8] *Photomultiplier Tubes: Basics and Applications.* Hamamatsu, 2006.